J Musculoskelet Neuronal Interact 2015; 15(4):316-324

Original Article

Hylonome

Differential effects of low-magnitude high-frequency vibration on reloading hind-limb soleus and gastrocnemius medialis muscles in 28-day tail-suspended rats

K-T. Sun[1], K-S. Leung[1], P.M-F. Siu[2], L. Qin[1,3], W-H. Cheung[1,3]

[1]Department of Orthopaedics and Traumatology, The Chinese University of Hong Kong, Shatin, New Territories, Hong Kong SAR;
[2]Department of Health Technology and Informatics, The Hong Kong Polytechnic University, Hung Hom, Kowloon, Hong Kong, China;
[3]The CUHK-ACC Space Medicine Centre on Health Maintenance of Musculoskeletal System,
The Chinese University of Hong Kong Shenzhen Research Institute, Shenzhen, The People's Republic of China

Abstract

Objectives: Low-magnitude high-frequency vibration (LMHFV) was reported beneficial to muscle contractile functions in clinical and preclinical studies. This study aims to investigate the effects of LMHFV on myofibers, myogenic cells and functional properties of disused soleus (Sol) and gastrocnemius medialis (GM) during reloading. **Methods:** Sprague Dawley rats were hind-limb unloaded for 28 days and assigned to reloading control (Ctrl) or LMHFV group (Vib). Sol and GM of both groups were harvested for fiber typing, proliferating myogenic cell counting and *in vitro* functional assessment. **Results:** Myogenic cells proliferation was promoted by LMHFV in both Sol and GM ($p<0.001$ and $p<0.05$ respectively). Force generating capacity was not much affected (Vib=Ctrl, $p>0.05$) but fast-fiber favorable changes in fiber type switching (more type IIA but lower type I in Vib; $p<0.05$ and 0.01 respectively) and fiber hypertrophy (type I, Vib<Ctrl; $p<0.01$) were observed mainly in GM. **Conclusion:** LMHFV was not detrimental to reloading muscles but the outcomes were muscle dependent. The unique fiber type composition and anatomical differences between Sol and GM might render the differential muscle responses to LMHFV. Further investigations on myofibers type specific responses to different LMHFV regimes and myogenic cell interaction with associated myofiber were proposed.

Keywords: Vibration, Skeletal Muscle, Reloading, Contractile Function, Fiber Type

Introduction

Skeletal muscles are highly mechanical sensitive and show high plasticity to altered activity levels[1-4]. Muscle disuse (or unloading), as in astronauts and bed-rest patients, leads to muscle atrophy and functional loss[5-6]. When designing treatment options for disuse atrophy, one must keep in mind that disused muscles are more susceptible to damage than normal muscles and hence over-exerting a disuse muscle may cause further deterioration, rather than improvement of muscle function[7-8].

Despite the numerous investigations on muscle disuse, less information about reloading from disuse and the suitable intervention is available. Moreover, most existing animal studies were conducted in a relatively short, 14-day tail suspension (TS) model and soleus muscle was the major muscle of interest. The duration of unloading and muscles of interests in fact are critical factors that lead to different degree of muscle-dependent, progressive physiological changes. For instance, myofibrillar protein loss was more prominent and became stable after 28 days of unloading than 7 and 14 days protocol whereas soleus was more affected than plantaris and gastrocnemius muscle (Details see Review by Thomason, 1990)[9-11]. A better understanding of the reloading effects on unloaded limb muscles will provide valuable information for determining safe and even customized intervention for the susceptible disused muscles during reloading.

Low-magnitude high-frequency vibration (LMHFV) is a

This study was funded by the General Research Fund (Ref: 469911) from the University Grants Committee, Hong Kong SAR, China.

Corresponding author: Wing-Hoi Cheung, Department of Orthopaedics and Traumatology, 5/F, Clinical Science Building, The Chinese University of Hong Kong, Shatin, New Territories, Hong Kong, China
E-mail: louis@ort.cuhk.edu.hk

Edited by: J. Rittweger
Accepted 10 July 2015

non-invasive biophysical modality, and its beneficial effects on musculoskeletal system are widely reported in various preclinical and clinical studies. Clinical trials showed that LMHFV prevented muscle atrophy in bed-rest patients and improved muscle performance with high compliance in community elderly[12-13]. Preclinical work from Xie and his colleague suggested vibration stimulated mice lower limbs muscle to hypertrophy[14]. Promoting proliferation and differentiation of myogenic cells as well as down-regulating genes involved in atrophy pathway could be the possible mechanisms of the muscle improvement by vibration treatment[15-16].

With the evidences of LMHFV effectiveness in muscle improvement, it was hypothesized that LMHFV improves the outcomes of reloading disused muscles. The objectives of the current study were to investigate the effects of LMFHV treatment on: 1) fiber morphology, 2) myogenic cells proliferation and, 3) contractile function of soleus (Sol) and gastrocnemius medialis (GM), two weight-bearing limb synergist muscles, during 21 days of reloading period. Given the lack of information about reloading from prolonged disuse, the current work would also demonstrate any differential outcomes of reloading on Sol and GM.

Materials and methods

Animal care and experimental design

A total of 48 6-month-old male *Sprague-Dawley* adult rats were obtained from the Laboratory Animal Service Centre of the Chinese University of Hong Kong. All animals were housed in temperature-controlled rooms with 12:12 hour dark-light cycle. All procedures performed in this study were approved by the Animal Experimentation Ethics Committee of the Chinese University of Hong Kong (Ref: 10/093/MIS5).

Animals were hind-limb unloaded for 28 days individually based on Morey's tail suspension (TS) protocol[17]. Briefly, zinc-oxide plaster with a harness was wrapped around the tail and secured by surgical tapes. Animals were then suspended in head-down position at torso-to-ground angle of ≤30°, while hind-limbs were dangled down without any solid support from the tail-suspension cage. Free-cage movement, access to water and standard rat chow *ad libitum* with their forelimbs were allowed. The health status of the animals was monitored daily. Age-matched weight bearing rats (WB, n=6) were euthanized at the same time for TS model verification.

After 28 days of TS, part of the unloading rats were sacrificed immediately (without reloading) and served as control of unloading (TS, or referred as Day 0 baseline data, n=6). The remaining rats were reloaded by allowing free-cage movement by four limbs in standard rat cage independently. The reloading rats were randomly assigned to either reloading control (Ctrl) or reloading plus vibration (Vib). Animals in Vib received LMHFV (0.6g, 35Hz; g=gravitational acceleration) 20 min/day and 5 days/week. Animals were euthanized by overdosed pentobarbital 7, 14 and 21 days after reloading (n=6/treatment/timepoint)[18]. Left Sol and GM were freshly harvested, weighted and subjected to *in vitro* functional assessment; the contralateral muscles were snap-frozen in melting isopentane, embedded in OCT compound and stored at -80°C until cryosectioning.

Proliferative cell labeling

To label proliferative cells in reloading muscles, a time-released pellet of 5-bromo-2'-deoxyuridine (BrdU, nucleotide analog to thymidine) (Innovative Research of America, FL, USA) was implanted subcutaneously 14 days before each endpoint[19]. Briefly, the animal was first anesthetized by isoflurane and according to manufacturer's instructions, the neck was shaved and disinfected by alcohol before a 5 mm longitudinal incision was made. A BrdU pellet was then put into a pocket 20 mm beyond the incision site subcutaneously. For the rats euthanized at Day 7 post-TS, BrdU pellet was implanted when the rats were still tail-suspended (i.e. day 21 of TS).

Histology

Consecutive 7μm cross-sections of right Sol and GM muscles were cut using cryostat. ATPase staining conditioned at pH 4.6 at room temperature was performed to distinguish the three muscle fibers: type I (darkest), IIA (lightest) and IIB (intermediate), based on Hintz's protocol and images of section were captured under the light microscope (Leica DFC490, Leica Microsystems)[20]. The whole section of Sol and the core region in the proximal head of GM (with mixed fibers profile) were analyzed[21]. Three random fields were captured to analyze the effects of LMHFV on different fiber types. The fiber cross-sectional area (FCSA) and the proportion (%) of fiber types I, IIA and IIB were measured with ImagePro Plus analysis software (v5.1.0.20, Media Cybernetics, MD, USA).

Immunohistochemistry

To identify proliferative myogenic cells and the associated fiber types in both Sol and GM, a BrdU/laminin double-staining protocol was performed on the ATPase stained cryosections as modified from Siu's protocol[19]. Primary antibodies included mouse anti-BrdU (1:100, Abcam) and rabbit anti-rat laminin (1:200, Abcam). Secondary antibodies included Alexa Fluor555-conjugated goat anti-mouse IgG (γ2a) secondary antibody (Zymed) and Alexa Fluor488-conjugated donkey anti-rabbit IgG(H+L) antibody working concentration at 4 μg/ml. BrdU-positive nuclei lying on the laminin-stained basement membrane were counted and considered as proliferative myogenic cells. Immunofluorescent images obtained were co-localized with ATPase staining to identify the fiber types that the proliferative myogenic cells associated with.

In vitro muscle functional assessment

The protocols for muscle functional assessment were modified from Plant and Segal's studies[22-23]. The distal tendon of muscle was sutured and hung onto the transducer (305C-LR, Aurora Scientific Inc.) with proximal end anchored to the *in vitro* functional test apparatus (805A, Aurora Scientific Inc.,

	Sol			GM		
Groups	**Mm (g)**	**pCSA (10^{-2} cm^2)**	**FCSA (10^3 μm^2)**	**Mm(g)**	**pCSA (10^{-2} cm^2)**	**FCSA (10^3 μm^2)**
TS (n=6)	0.200 ± 0.017 [a]	6.20 ± 0.62 [a]	2.87± 0.12 [a]	1.164 ± 0.090 [a]	25.68 ± 2.55 [a]	2.59 ± 0.20 [a]
WB (n=6)	0.300 ± 0.024	8.85 ± 0.94	4.74 ± 0.31	1.556 ± 0.100	33.14 ± 2.07	4.57 ± 0.63

Table 1. The ***Sol*** (Left column) and ***GM*** (Right column) muscle mass (Mm), physiological cross-sectional area (pCSA) and fiber cross-sectional area (FCSA) between weight-bearing group (WB) and hind-limb unloading group (TS) (n=6, mean ± SD). [a] WB larger than TS, p<0.001 by independent samples t-test.

Ontario, Canada). Muscles were stimulated to contract by square-wave pulses (0.2 ms width) at supramaximal voltage (80V). The detected forces were recorded by Dynamic Muscle Control (DMC v5.1) and analyzed with Dynamic Muscle Analysis (DMA v3.2) software (Aurora Scientific Inc.). All muscles were isometrically stimulated at optimal length (Lo) at room temperature (around 25°C in air-conditioned laboratory) which was determined by eliciting isometric twitch with increasing muscle length until maximal force was generated[22].

For Sol, force-frequency relationship was determined by stimulating the muscle for 1s at 10, 20, 40, 60, 80 and 100 Hz with 5-minute resting intervals. Maximal tetanic force of Sol was defined as the largest force obtained from the force-frequency relationship. For GM, continuous tetanic stimulation was unfavorable due to potential core anoxia induced by poor oxygen/nutrient perfusion to the bulky GM that deteriorated contractile function and would lead to severe force underestimation. Hence, isometric tetanic force of GM was achieved by delivering supramaximal stimulation, 500 ms, 150Hz at optimal length once only. All force measurement was normalized by physiological cross-sectional area (pCSA). It was estimated by pCSA= mass (g)/[muscle length (cm) x muscle density (gcm^{-3})], where muscle density is assumed as 1.056 (gcm^{-3})[24].

Statistical analysis

All data were expressed in mean ± standard deviation. Two-way analysis of variance (ANOVA) test was applied to analyze the main effects amongst treatment and reloading period. Post-hoc multiple comparison corrected by Bonferroni adjustment was performed when significant main effects were detected. When significant interaction was detected, independent Student's t-test were used for further comparisons between Vib and Ctrl groups. All statistical analyses were performed with SPSS 20.0 (IBM, NY, USA). Statistical significance was set at $p<0.05$.

Results

TS model verification

The Sol muscle mass (Mm), pCSA and FCSA were significantly decreased by 33%, 31% and 40% respectively in TS group whereas in GM, these were decreased by 26%, 23% and 43% respectively (*all* p< 0.001; Table 1). Muscle fibers atrophy and slow-to-fast fiber type transition could be observed in both Sol and GM. Besides, increase in interstitial space in TS was observed (Figure 1).

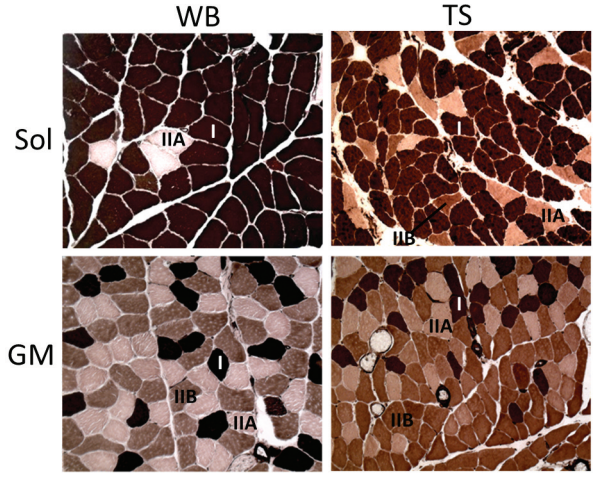

Figure 1. Typical ATPase (pH4.6) staining images of weight bearing (**WB**, left column) and unloading (**TS**, right column) from soleus (***Sol***, upper panel) and gastrocnemius medialis (**GM,** lower panel). Type I (I, darkest), type IIA (IIA, lightest) and type IIB (IIB, intermediate) were indicated. *Note that no type IIB in Sol WB (upper left). Magnification: 200X.

Muscle morphology

The morphological data of Sol and GM muscles in Ctrl and Vib groups at different reloading period were summarized in Tables 2 and 3 respectively. Reloading induced an increase in most of the morphological outcomes during reloading but differential responses to reloading and LMHFV treatment could be observed between Sol and GM. Particularly, decrease of Lo (~3%, p<0.05) during reloading compared with TS and smaller overall FCSA (Vib<Ctrl; p<0.01) in LMHFV group could only be observed in GM. Instead, Lo of Sol increased with reloading compared with TS (~7%, p<0.05) and LMHFV treatment did not demonstrate any effects on Sol overall FCSA (Vib=Ctrl; p>0.05). Other morphological parameters including muscle mass (~35%, p<0.001), pCSA (~28%, p<0.001) and FCSA (~27%, p<0.01) increased in Sol during reloading and

Group/ Timepoint		Sol			
		Mm (g)	Lo (cm)	pCSA (10^{-2} cm^2)	FCSA (10^3 μm^2)
TS		0.200 ± 0.017 [b,d,f,h]	3.06 ± 0.11 [e]	6.20 ± 0.62 [b,d,f,h]	2.87 ± 0.12 [a,c,g]
Day 7	**Ctrl**	0.221 ± 0.034	2.89 ± 0.10	7.21 ± 1.00	3.51 ± 0.58
	Vib	0.226 ± 0.021	3.01 ± 0.08	7.09 ± 0.68	3.37 ± 0.17
Day 14	**Ctrl**	0.268 ± 0.017	3.10 ± 0.16	8.40 ± 0.87	3.86 ± 0.27
	Vib	0.268 ± 0.007	3.09 ± 0.10	8.20 ± 0.16	3.44 ± 0.23
Day 21	**Ctrl**	0.273 ± 0.025	3.34 ± 0.02	7.84 ± 0.71	3.25 ± 0.31
	Vib	0.271 ± 0.015	3.21 ± 0.16	7.97 ± 0.56	3.49 ± 0.41

Table 2. Morphological data summary of ***Sol*** from TS, Ctrl and Vib at different timepoints including muscle mass (Mm), optimal length (Lo), physiological cross-sectional area (pCSA) and fiber cross-sectional area (FCSA). [a,b] Ctrl larger than TS, p<0.01 and p<0.001 respectively; [c,d] Vib larger than TS, p<0.05 and p<0.001 respectively; [e,f] Day21 larger than TS, p<0.05 and p<0.001 respectively; [g,h] Day 14 larger than TS, p<0.01 and p<0.001; main effects detected from Two-way ANOVA. No significant interaction detected.

Group/ Timepoint		GM			
		Mm (g)	Lo (cm)	pCSA (10^{-2} cm^2)	FCSA (10^3 μm^2)
TS		1.164 ± 0.100 [a,d,e,g]	4.30 ± 0.08 [f]	25.68 ± 2.55 [b,d,e,f]	2.59 ± 0.20 [b,c,e]
Day 7	**Ctrl**	1.195 ± 0.091	4.12 ± 0.10	27.44 ± 2.05	3.05 ± 0.21
	Vib	1.213 ± 0.063	4.24 ± 0.08	27.13 ± 1.28	3.09 ± 0.32
Day 14	**Ctrl**	1.386 ±0.107	4.09 ± 0.16	32.10 ± 2.12	3.06 ± 0.16
	Vib	1.376 ±0.132	4.21 ± 0.10	30.07 ± 1.58	2.62 ± 0.21
Day 21	**Ctrl**	1.403 ± 0.049	4.38 ± 0.03	30.43 ± 1.20	3.79 ± 0.35 [h]
	Vib	1.426 ± 0.112	4.34 ± 0.05	30.34 ± 1.48	3.27 ± 0.33

Table 3. Morphological data summary of ***GM*** from TS, Ctrl and Vib at different timepoints including muscle mass (Mm), optimal length (Lo), physiological cross-sectional area (pCSA) and fiber cross-sectional area (FCSA). [a,b] Ctrl larger than TS, p<0.01 and p<0.001 respectively; [c,d] Vib larger than TS, p<0.05 and p<0.01 respectively; [e] Day21 larger than TS, p<0.001; [f] TS larger than Day 14, p<0.05; [g] Day 14 larger than TS, p<0.001; [h] Ctrl larger than Vib, p<0.01; main effects detected from Two-way ANOVA. No significant interaction detected.

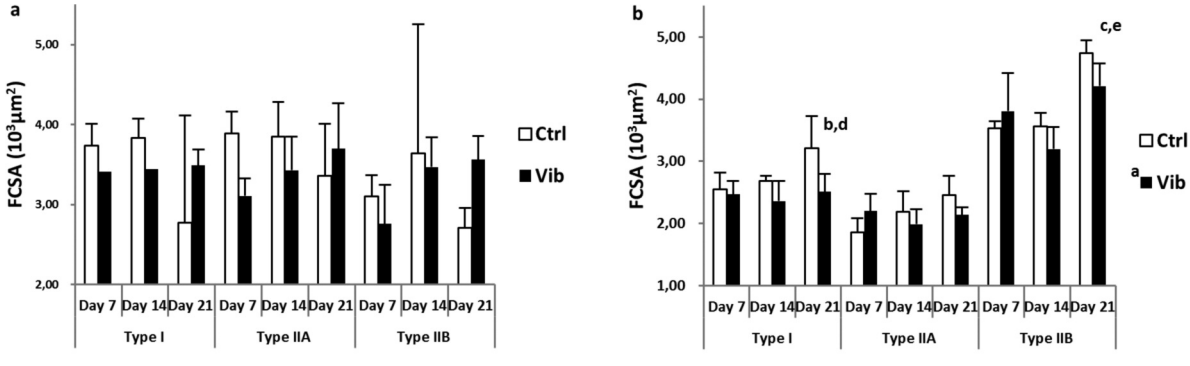

Figure 2. Fiber cross-sectional area (FCSA) (10^3 μm^2) of three fiber types: type I, IIA and IIB from pH4.6 ATPase staining. **a)** soleus (***Sol***): No significant difference detected amongst all comparisons; **b)** gastrocnemius medialis (**GM**): [a] Reloading control (Ctrl) larger than reloading plus vibration (Vib) in type I FCSA, p<0.01; [b,c] Day 21 larger than Day 7, p<0.01 and p<0.001 respectively; [d,e] Day 21 larger than Day 14, p<0.01 and p<0.001 respectively; main effects detected from Two-way ANOVA coupled with post-hoc Bonferroni adjustment. No significant interaction detected.

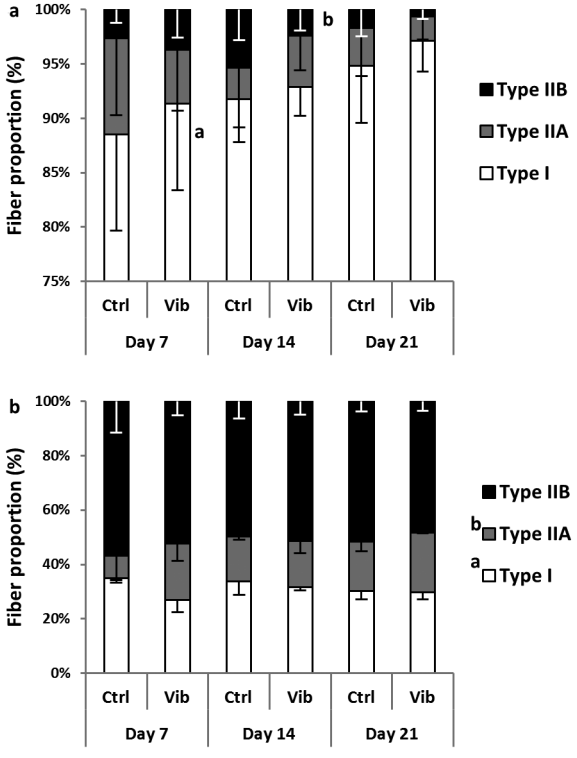

Figure 3. The proportion (%) of three fiber types, type I, IIA and IIB from pH4.6 ATPase staining. **a)** soleus (***Sol***): [a] higher % type I in Day 21 than Day 7, p = 0.05; [b] lower % type IIB in Day 21 than Day 14, p<0.05; **b)** gastrocnemius medialis (***GM***): [a] higher % type I in reloading control (Ctrl) than reloading plus vibration (Vib), p<0.01 (interaction, p<0.05); [b] higher % type IIA in Vib than Ctrl, p<0.05 (interaction, p=0.05); main effects and interaction detected from Two-way ANOVA coupled with post-hoc Bonferroni test.

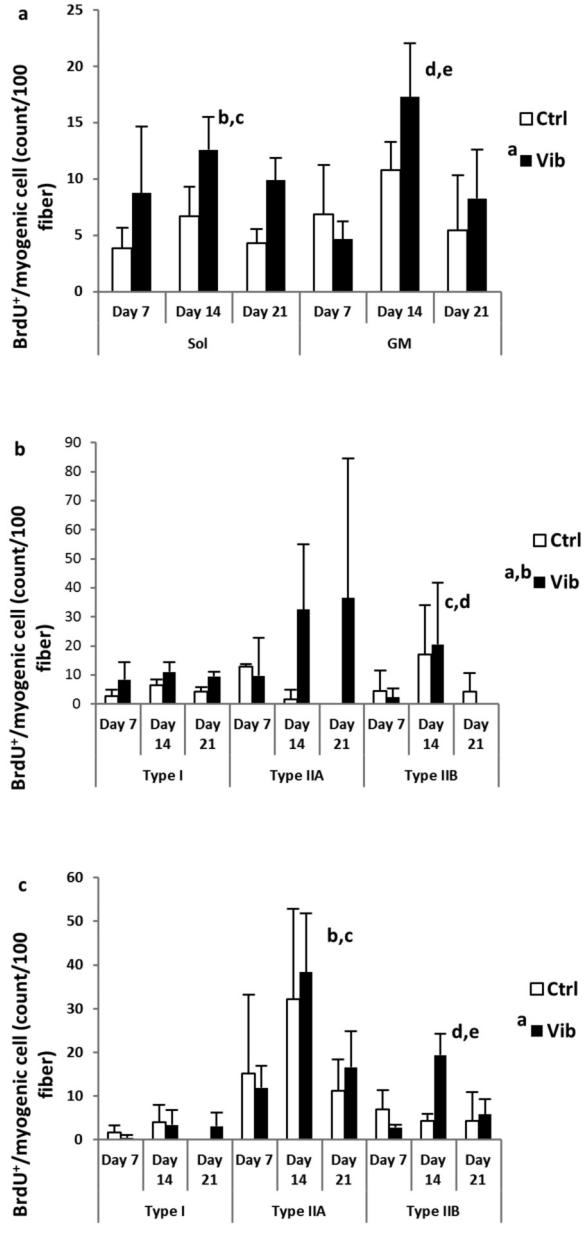

Figure 4. Proliferating myogenic cell counts (count / 100 fibers) from soleus (Sol) and gastrocnemius medialis (GM) muscles. **a) overall** bromodeoxyuridine (BrdU)+/myogenic cell in ***Sol*** (left panel) and ***GM*** (right panel). [a] Reloading plus vibration (Vib) more than reloading control (Ctrl) in Sol, p<0.001; [b] Day 14 more than Day 7 in Sol, p<0.05; [c] Day 14 more than Day 21 in Sol, p=0.052; [d] Day 14 more than Day 7 in GM; [e] Day 14 more than Day 21 in GM, p<0.001; **b) *Sol*:** fiber type specific BrdU+/myogenic cell associated with type I, IIA and IIB fibers. [a] Vib more than Ctrl in type I, p<0.05; [b] Vib more than Ctrl in type IIA, p< 0.05; [c] Day 14 > Day 7 in type IIB, p<0.001; [d] Day 14 > Day 21 in type IIB, p<0.001; **c) *GM*:** fiber type specific BrdU+/myogenic cell associaed with type I, IIA and IIB fibers. [a] Vib more than Ctrl in type IIB, p<0.05 (interaction, p<0.001); [b] Day 14 > Day 7 in type IIA, p<0.01; [c] Day 14 > Day 21 in type IIA, p<0.01; [d] Day 14 > Day 7 in type IIB, p<0.01; [e] Day 14 > Day 21 in type IIB, p<0.001; main effects and interaction detected from Two-way ANOVA coupled with post-hoc Bonferroni test.

similarly in GM with muscle mass (~23%, p<0.001), pCSA (~17%, p<0.001) and FCSA (~26%, p<0.001), all compared with the corresponding value in TS.

Fiber typing - FCSA and fiber proportion

The changes of FCSA of different fiber types (type I, IIA and IIB) in Sol and GM were illustrated in Figure 2a and 2b respectively. Fiber-type specific FCSA of Sol were similar and no difference (p>0.05) was detected during reloading (Figure 2a), whereas GM showed significant increase at Day 21 compared with Day 7 and Day 14 in type I (both p<0.01) and type IIB fibers (both p<0.001) (Figure 2b). Besides, Ctrl type I FCSA, but not type IIA or IIB, of GM was larger than that of Vib (p<0.01) and echoed with the overall FCSA decrease in Vib.

For the fiber type proportion, the percentage of all fiber types in Sol and GM were illustrated in Figures 3a and 3b respectively. Sol was made up of >90% type I fibers and increasing trend of type I percentage was observed during reloading (Day 21>Day 7, p=0.052). On the contrary, Sol type IIB percentage decreased from Day 14 to Day 21 significantly

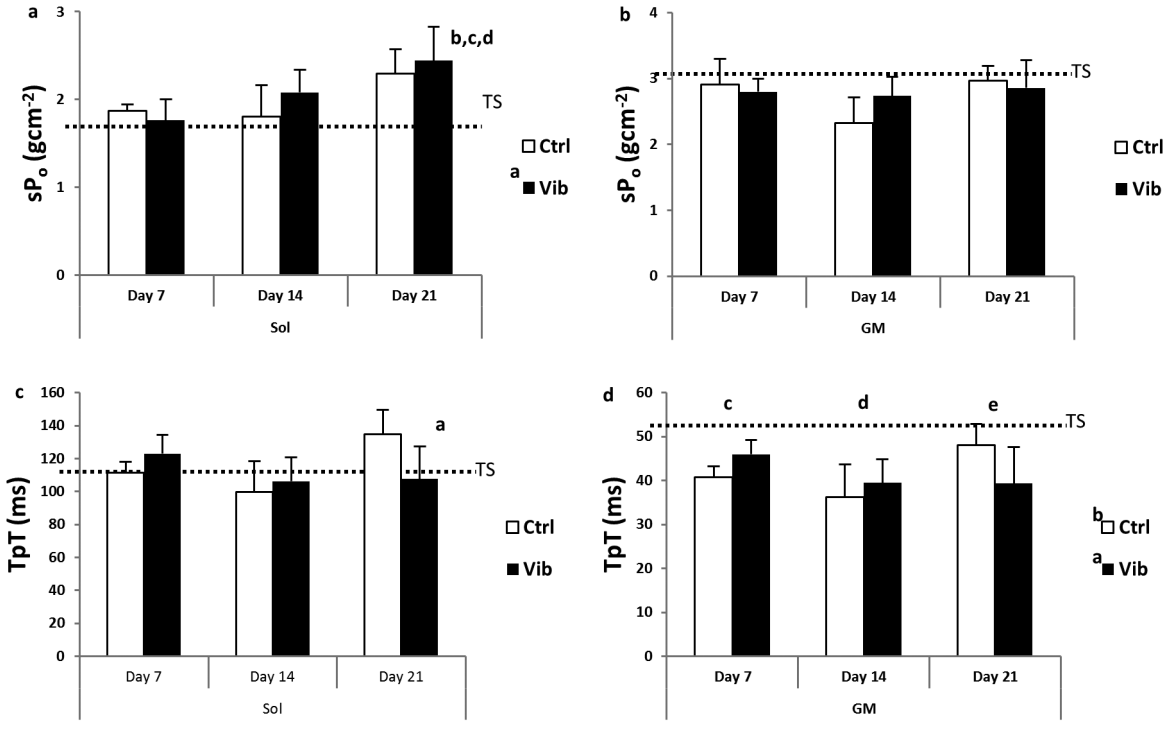

Figure 5. Contractile properties - specific force (**sP_o**, gcm^{-2}) and contraction time to peak twitch (TpT, ms) of soleus (**Sol**) and gastrocnemius medialis (**GM**) during reloading. The dotted line in each graph was the corresponding mean in unloading (**TS**) group. **a) sP_o - Sol:** [a] reloading plus vibration (Vib) larger than TS, $p<0.05$; [b] Day 21 larger than TS, $p<0.001$; [c] Day 21 larger than Day 7, $p<0.001$; [d] Day 21 larger than Day 14, $p<0.01$; **b) sP_o - GM:** a Day 21 larger than Day 14, $p<0.05$; **c) TpT - Sol:** [a] Day 21 slower than Day 14, $p<0.05$ (interaction, $p<0.01$); **d) TpT - GM:** [a] reloading control (Ctrl) faster than TS, $p<0.001$; [b] Vib faster than TS, $p<0.001$; [c] Day 7 faster than TS, $p<0.05$; [d] Day 14 faster than TS, $p<0.001$; [e] Day 21 faster than TS, $p<0.05$; main effects and interaction detected from Two-way ANOVA coupled with post-hoc Bonferroni test.

($p<0.05$). Vibration treatment showed no effects on Sol fiber types switching.

Regarding GM fiber percentage, GM was composed of a mix of three fiber types with type IIB constituting ~50% of the total fibers in the core region of GM. Different from Sol, fiber type transition during reloading was absent in GM. Comparing Ctrl and Vib, there was a higher type I proportion in Ctrl ($p<0.01$; interaction with $p<0.05$) whereas type IIA was higher in Vib ($p<0.05$; treatment*timepoints interaction with $p=0.05$). Significant interactions were found in these two main effects i.e. reloading time and treatment. Therefore post-hoc test was carried out to compare the differences between Ctrl and Vib across timepoints. The post-hoc independent t-test analysis showed a higher type I proportion in Ctrl at Day 7 (Ctrl>Vib, $p<0.01$) whereas that for type IIA proportion was higher in Vib at Day 7 (Vib>Ctrl, $p<0.05$) and Day 21 (Vib>Ctrl, $p=0.05$).

Proliferating myogenic cell counting

The counting results were illustrated in Figure 4 (a-c). The Vib group generally showed higher counting in both Sol and GM. Overall counting, and fiber type specific counts in type I and IIA in Sol were higher in Vib than Ctrl (all $p<0.001$, Figures 4a and 4b). Although overall counting showed no difference between Vib and Ctrl in GM, fiber type specific counting revealed higher counts in type IIB fiber of Vib group ($p<0.05$, Figure 4c). Significant treatment*timepoints interaction ($p<0.001$) was detected in this observable increase of myogenic cells proliferation in Vib during reloading. The post-hoc independent t-tests showed that the increase of type IIB count in Vib was at Day 14 (Day 14-Vib>Day 14-Ctrl, $p<0.001$) while the other two timepoints had no differences.

Moreover, the peak counting during reloading period was at Day 14 in all three fiber types. The counts actually covered all the proliferative activities happened from day 0 to day 14 of reloading (See Method for details). The time of peak activity was apparently independent of the fiber types, treatment and muscles of interest (except type IIA in Sol which the counts maintained high in Vib, see Figure 4b).

Contractile properties - specific force (sP_o) and time to peak twitch (TpT)

The contractile properties of Sol and GM were illustrated in Figure 5 (a-d). Increase in sP_o during reloading was observed in Sol (Figure 5a; Day 21>TS and Day 7, both $p<0.001$ and

Day 14, $p<0.01$) while force deficit, compared to TS level, was evident in GM throughout the reloading period in spite of the increasing trend from Day 14 to Day 21 (Figure 5b; $p<0.05$). LMHFV treatment appeared promoting force generating capacity in Sol as indicated from higher sP_o in Vib compared with TS (Vib>TS, $p<0.05$) which was, however, absent in Ctrl (Figure 5a). GM sP_o in Vib was not different from the Ctrl nor the TS. The contraction time, TpT of Sol appeared longer at Day 21 as compared with Day 14. Nevertheless, given a significant interaction detected ($p<0.01$), further post-hoc comparison showed that TpT of Ctrl-Day 21 was significantly longer than Vib-Day21 ($p<0.05$) and TS ($p<0.01$) (Figure 5c). As for GM, TpT decreased and was significantly shorter than TS during the reloading period. Otherwise, the changes of TpT amongst all comparisons between Vib and Ctrl or among timepoints were not different significantly ($p>0.05$) (Figure 5d).

Discussion

The current study aims to examine the effects of LMHFV intervention on the regrowth process of reloading muscles from prolonged disuse at functional, histo-morphological and cellular levels. The results showed LMHFV intervention was not injurious to reloading muscles, both Sol and GM, while myogenic cells proliferative activities were enhanced. Only in the GM demonstrated type I fiber hypertrophy and a type I to type IIA fiber transition was observed upon LMHFV treatment during reloading. Further investigations on the fiber type specific responses of various muscles toward LMHFV and interaction of myogenic cells with the associated myofiber were recommended.

The 28-day tail suspension prolonged muscle disuse model (TS) in rat was applied to investigate the effects of LMHFV treatment on two reloading lower limbs muscles, Sol and GM. It was well known slow-twitch muscle fibers were more susceptible to disuse atrophy compared with the fast counterparts[9-10]. Hence differential influences of 28-day TS on Sol (slow-dominant) and GM (fast-dominant except the mixed core region) should be expected. Our results were consistent with the previous findings that the gross morphology of Sol was reduced more than that of GM in response to TS[25-26]. For FCSA, the changes appeared similar between Sol and the core region of GM. The peripheral region of GM, in fact composed mainly of type IIB fibers, showed no changes in FCSA within the region (data not shown). Hence, if whole GM was considered, the effects of TS on GM were not as prominent as in Sol. This intrinsic difference should be taken into consideration in interpreting the differential responses of Sol and GM to reloading.

In Sol, reloading regrowth could be observed from morphological (gain of Mm, Lo, and pCSA) and fiber typing data (increased FCSA and fast-to-slow type transition). Coupled with functional data, the increasing specific sP_o and longer TpT, reloading induced regrowth of Sol was evident and consistent with previous report[8]. Furthermore, it was apparent that Vib promoted gain of force generating capacity as indicated from the significantly higher sP_o compared with TS. This increasing trend, nevertheless, was not significant in Ctrl. Longer timepoints of Vib treatment may allow a clearer picture of this beneficial effect. Comparing with Sol, the case in GM was rather more complicated. Although Mm, pCSA and FCSA increased during reloading suggesting apparent muscle regrowth, Lo decreased at the early timepoints and specific force deficit in GM was observed during the whole reloading period. This deficit was neither be improved nor deteriorated by LMHFV. To explain the deficit, reloading induced injury in GM was suggested[8].

Reloading injury is caused by myofiber disruption due to stretching or increased muscle strain when the shortened disused myofibers were reloaded and lengthened. It was known that TS unloaded muscle fibers were shortened to adapt to the prolonged plantar flexion of the foot, which was typically observed in prolonged TS model[27]. In addition, the anatomy of gastrocnemius muscle which connects two joints (ankle and knee) and is composed of fast-fibers in majority may render its higher susceptibility toward eccentric/ stretching injury during reloading than Sol[8,28]. It might explain our current findings that GM showed a prolonged functional deficit during reloading even it was less affected by unloading than Sol[28]. Given Sol also experienced fiber shortening, it was expected to be affected by reloading injury and demonstrated force deficit. Previous studies showed the onset of force decrement in Sol was around 1-2 days from reloading and the weakness may last no longer than 9 days[8,29]. Our results did not contradict with these findings that force generating capacity remained similar to TS (no increase) at Day 7 (the earliest timepoint of this study) and an increase could be observed since Day 14. In summary, LMHFV have mild effects on Sol functional recovery and is non-injurious to mechanical injury-prone GM during reloading. Optimization of LMHFV treatment period might enhance the beneficial outcomes and lead to significant difference from Ctrl in Sol without adverse effects on GM.

Myogenic cell proliferative activities were found elevated by counting overall myogenic cells regardless of the associated fiber types in Sol only. In addition to overall counting, the current investigation adopted the novel fiber type specific myogenic cell analysis to evaluate the effects of LMHFV on myogenic cell activities. The concept of fiber associated myogenic cell progeny was suggested from Verdijk's group including reduced satellite cells in aging type II skeletal muscle fibers and increased SC counts in type II fibers after eccentric exercises[30-31]. The effects of LMHFV on fiber-type specific counts were found in both Sol (type I and IIA) and GM (type IIB). Stimulatory effects of LMHFV on myogenic cells proliferation were therefore evident in both Sol and GM. This indicated that the analysis of overall myogenic cell activities might underestimate or even misinterpret the effects of particular intervention.

Referring to Verdijk's studies, the fiber type specific changes could be primary to the vulnerable type II fibers in eccentric and aging models[30-31]. Hence it was questionable if the fiber type specific effects observed in this study were related to fiber susceptibility to injury. Our functional results showed vibration was not injurious to Sol and even in the mechanical sensitive GM. Instead, trend of faster force regain in Sol was found. Similarly, administration of vibration of similar

regime (45 Hz, 0.6 g) on dystrophic mice model, with skeletal muscles well-known susceptible to mechanical damages, showed no detrimental effects as well[32]. Hence damages to muscle cells by vibration treatment should be absent or negligible, if any. In the same study, 7 days of treatment could upregulate muscle paired box gene-7 (Pax7) gene expression, a myogenic cell marker particularly in quiescent muscle satellite cell, which suggested promotion of myogenic cells activities *in vivo*[32]. *In vitr*o vibration treatment on myogenic cell line, C2C12, was also reported to increase cell proliferation and myogenic differentiation without any injury or challenge to the cultured cells[15]. Therefore, it was conceived to regard the current findings primarily as direct promotion of myogenic cell proliferation and less likely related to induced myofiber injury. However, it remained questionable why myogenic cells associated with particular fiber types appeared more responsive to LMHFV. Recruitment of different kinds of motor units during vibration treatment, according to tonic vibration reflex (TVR) was evident and suggested only fibers under the activated motor units responded to contract[33-35]. Besides, communication mechanisms between the associated myofibers and adjacent myogenic cells have been reported[36-37]. It implied the possibility that LMHFV might trigger specific types of fiber to contract and stimulate the associated myogenic cell activities leading to the fiber type specific myogenic cell responses. More speculations on interaction of myogenic cells and the associated fibers upon mechanical stimuli are suggested.

In addition to stimulation of type IIB myogenic cells activities, LMHFV induced fast fiber type specific effects on other outcomes of GM, for instance, suppression of type I fiber hypertrophy and shift of type IIA fibers from type I counterparts. A trend of shorter TpT at Day 21 could be observed in GM as well. LMHFV hence apparently favored GM fast fiber changes during reloading. It was interesting that Sol showed increases in both type I and IIA associated myogenic cell activities. Also, Xie's study showed vibration stimulated both type I and type IIA fiber hypertrophy in growing mice[14]. Although fast-to-slow fiber type transition in Sol was not affected by LMHFV, significantly shorter TpT was detected. It was unclear if other factors like calcium handling and cross-bridge kinetics attributed to the difference. In general, the fiber type specific responses appeared muscle-dependent. It was worthy for further investigations on the differential responses of the two muscles to various vibration regimes (e.g. changes in frequency and magnitude) and to examine the fiber type specific changes.

In conclusion, LMHFV intervention did no harm on the contractile functions of reloading muscles during 21 days of reloading while myogenic cell activities could be promoted in both Sol and GM. However, a limitation of the current study was that the cell fate of the increased number of myogenic cells was uncertain. It remains to be seen whether the fiber type specific changes due to LMHFV were dependent on the elevated myogenic cell activity. The reloading effects on Sol and GM were different and the concerns of customizing intervention for particular muscles should be well-considered so that therapeutic effects were maximized without compromising other muscles toward injury. The use of LMHFV in treating prolonged disused muscles should be further investigated to depict the regulatory mechanisms of the myofibers on the associated myogenic cells as well as the fiber type specific responses in different LMHFV regimes.

Acknowledgements

We would like to thank Prof. Anthony Bakker, The University of Western Australia, for his technical experience and support in in vitro functional assessment.

References

1. Blazevich AJ. Effects of physical training and detraining, immobilisation, growth and aging on human fascicle geometry. Sports Med 2006;36:1003-1017.
2. Fluck M, Hoppeler H. Molecular basis of skeletal muscle plasticity - from gene to form and function. Rev Physiol Biochem Pharmacol 2003;146:159-216.
3. Fluck M. Functional, structural and molecular plasticity of mammalian skeletal muscle in response to exercise stimuli. J Exp Biol 2006;209:2239-2248.
4. Hoppeler H, Fluck M. Normal mammalian skeletal muscle and its phenotypic plasticity. J Exp Biol 2002; 205:2143-2152.
5. Droppert PM. A review of muscle atrophy in microgravity and during prolonged bed rest. J Br Interplanet Soc 1993; 46:83-86.
6. Mercier C, Jobin J, Lepine C, Simard C. Effects of hindlimb suspension on contractile properties of young and old rat muscles and the impact of electrical stimulation on the recovery process. Mech Ageing Dev 1999; 106:305-320.
7. Frenette J, St-Pierre M, Cote CH, Mylona E, Pizza FX. Muscle impairment occurs rapidly and precedes inflammatory cell accumulation after mechanical loading. Am J Physiol Regul Integr Comp Physiol 2002;282:R351-357.
8. Widrick JJ, Maddalozzo GF, Hu H, Herron JC, Iwaniec UT, Turner RT. Detrimental effects of reloading recovery on force, shortening velocity, and power of soleus muscles from hindlimb-unloaded rats. Am J Physiol Regul Integr Comp Physiol 2008;295:R1585-1592.
9. Thomason DB, Herrick RE, Surdyka D, Baldwin KM. Time course of soleus muscle myosin expression during hindlimb suspension and recovery. J Appl Physiol 1987;63:130-137.
10. Thomason DB, Booth FW. Atrophy of the soleus muscle by hindlimb unweighting. J Appl Physiol (1985) 1990; 68:1-12.
11. Hanson AM, Harrison BC, Young MH, Stodieck LS, Ferguson VL. Longitudinal characterization of functional, morphologic, and biochemical adaptations in mouse skeletal muscle with hindlimb suspension. Muscle Nerve 2013;48:393-402.
12. Moriggi M, Vasso M, Fania C, Capitanio D, Bonifacio G, Salanova M, Blottner D, Rittweger J, Felsenberg D, Cer-

retelli P, Gelfi C. Long term bed rest with and without vibration exercise countermeasures: effects on human muscle protein dysregulation. Proteomics 2010;10:3756-3774.
13. Leung KS, Li CY, Tse YK, Choy TK, Leung PC, Hung VW, Chan SY, Leung AH, Cheung WH. Effects of 18-month low-magnitude high-frequency vibration on fall rate and fracture risks in 710 community elderly - a cluster-randomized controlled trial. Osteoporos Int 2014; 25:1785-1795.
14. Xie L, Rubin C, Judex S. Enhancement of the adolescent murine musculoskeletal system using low-level mechanical vibrations. J Appl Physiol 2008;104:1056-1062.
15. Wang CZ, Wang GJ, Ho ML, Wang YH, Yeh ML, Chen CH. Low-magnitude vertical vibration enhances myotube formation in C2C12 myoblasts. J Appl Physiol 2010; 109:840-848.
16. Ceccarelli G, Benedetti L, Galli D, Pre D, Silvani G, Crosetto N, Magenes G, Cusella De Angelis MG. Low-amplitude high frequency vibration down-regulates myostatin and atrogin-1 expression, two components of the atrophy pathway in muscle cells. J Tissue Eng Regen Med 2014;8:396-406.
17. Morey-Holton ER, Globus RK. Hindlimb unloading rodent model: technical aspects. J Appl Physiol 2002; 92:1367-1377.
18. Chow DH, Leung KS, Qin L, Leung AH, Cheung WH. Low-magnitude high-frequency vibration (LMHFV) enhances bone remodeling in osteoporotic rat femoral fracture healing. J Orthop Res 2011;29:746-752.
19. Siu PM, Pistilli EE, Butler DC, Alway SE. Aging influences cellular and molecular responses of apoptosis to skeletal muscle unloading. Am J Physiol Cell Physiol 2005;288:C338-349.
20. Hintz CS, Coyle EF, Kaiser KK, Chi MM, Lowry OH. Comparison of muscle fiber typing by quantitative enzyme assays and by myosin ATPase staining. J Histochem Cytochem 1984;32:655-660.
21. Wang LC, Kernell D. Proximo-distal organization and fibre type regionalization in rat hindlimb muscles. J Muscle Res Cell Motil 2000;21:587-598.
22. Plant DR, Beitzel F, Lynch GS. Length-tension relationships are altered in regenerating muscles of the rat after bupivacaine injection. J Appl Physiol 2005;98:1998-2003.
23. Segal SS, Faulkner JA. Temperature-dependent physiological stability of rat skeletal muscle *in vitro*. Am J Physiol 1985;248:C265-270.
24. Payne AM, Dodd SL, Leeuwenburgh C. Life-long calorie restriction in Fischer 344 rats attenuates age-related loss in skeletal muscle-specific force and reduces extracellular space. J Appl Physiol (1985) 2003;95:2554-2562.
25. Jain PK, Banerjee PK, Baboo NS, Iyer EM. Physiological properties of rat hind limb muscles after 15 days of simulated weightless environment. Indian J Physiol Pharmacol 1997;41:23-28.
26. Tischler ME, Henriksen EJ, Munoz KA, Stump CS, Woodman CR, Kirby CR. Spaceflight on STS-48 and earth-based unweighting produce similar effects on skeletal muscle of young rats. J Appl Physiol (1985) 1993;74:2161-2165.
27. Riley DA, Slocum GR, Bain JL, Sedlak FR, Sowa TE, Mellender JW. Rat hindlimb unloading: soleus histochemistry, ultrastructure, and electromyography. J Appl Physiol (1985) 1990;69:58-66.
28. Bryan Dixon J. Gastrocnemius vs. soleus strain: how to differentiate and deal with calf muscle injuries. Curr Rev Musculoskelet Med 2009;2:74-77.
29. Pottle D, Gosselin LE. Impact of mechanical load on functional recovery after muscle reloading. Med Sci Sports Exerc 2000;32:2012-2017.
30. Verdijk LB, Koopman R, Schaart G, Meijer K, Savelberg HH, van Loon LJ. Satellite cell content is specifically reduced in type II skeletal muscle fibers in the elderly. Am J Physiol Endocrinol Metab 2007;292:E151-157.
31. Cermak NM, Snijders T, McKay BR, Parise G, Verdijk LB, Tarnopolsky MA, Gibala MJ, Loon LJ. Eccentric Exercise Increases Satellite Cell Content in Type II Muscle Fibers. Med Sci Sports Exerc 2013;45:230-237.
32. Novotny SA, Eckhoff MD, Eby BC, Call JA, Nuckley D, Lowe DA. Musculoskeletal response of dystrophic mice to short term, low intensity, high frequency vibration. J Musculoskelet Neuronal Interact 2013;13:418-429.
33. Pollock RD, Woledge RC, Martin FC, Newham DJ. Effects of whole body vibration on motor unit recruitment and threshold. J Appl Physiol (1985) 2012;112:388-395.
34. Delecluse C, Roelants M, Verschueren S. Strength increase after whole-body vibration compared with resistance training. Med Sci Sports Exerc 2003;35:1033-1041.
35. Martin BJ, Park HS. Analysis of the tonic vibration reflex: influence of vibration variables on motor unit synchronization and fatigue. Eur J Appl Physiol Occup Physiol 1997;75:504-511.
36. Bischoff R. Interaction between satellite cells and skeletal muscle fibers. Development 1990;109:943-952.
37. Tavi P, Korhonen T, Hanninen SL, Bruton JD, Loof S, Simon A, Westerblad H. Myogenic skeletal muscle satellite cells communicate by tunnelling nanotubes. J Cell Physiol 2010;223:376-383.